Chapter 4

Numerical Investigation of the Effect of Swirl Strength, Combustion Environment, Inlet Temperature and Pressure of Feed gas on Flow and Combustion Characteristics

4.1 Overview

In this chapter, the effect of important operating parameters such as swirl strength, combustion environment, inlet temperature and pressure of feed gas on the flow field and combustion characteristics has been investigated. A quantitative analysis showing the effect of swirl strength, various combustion environment, inlet temperature and pressure of feed gas on the length of internal recirculation zone (IRZ) and the flame front has also been discussed in this chapter. Furthermore, the influence of various combustion environment on the temporal variation of particle-phase variables such as particle temperature, particle volatile and particle char mass fraction has also studied in this chapter.

4.2 Effect of Swirl Strength

Under this section, the effect of swirl strength on the flow field and combustion characteristics under oxy-fuel combustion conditions is discussed in detail. Secondary stream swirl number is varied, keeping feed gas flow rate constant. The swirl numbers used in the investigation are (a) 0.06 (b) 0.57 (c) 1.0 (d) 1.25. All the investigations are

performed under base oxy-fuel combustion environment for which experimental validation has been discussed.

4.2.1 Flow Field Distribution

Fig. 4.1. displays the contour of axial velocity along with the streamlines for different swirl numbers. An increase in swirl strength resulted in an enhancement in both the length and the intensity of internal recirculation zone created along the axis of furnace. At higher swirl strength, the higher negative pressure created near the burner causes the formation of a strong recirculation zone. The strong internal recirculation zone suppressed the axial dispersion of flame and flame spreads out in the radial direction. Longer internal recirculation zone (IRZ) also shapes the flames by making flames shorter and wider. An increase in swirl number resulted in reduced external recirculation zone. As swirl number is increased from 1.0 to 1.25, the change in the axial velocity contour is marginal.

Fig. 4.2 shows the radial variation of axial velocity at axial locations 0.05 and 0.2 m from the burner outlet for different swirl numbers. From the figure, it can be noted that at axial locations 0.05 m, the maximum axial velocity is obtained at a radial position of 0.05 m for all four swirl numbers. Swirl number 1.25 has the highest peak of axial velocity, whereas swirl number 0.06 has the lowest peak. As the swirl number is increased from 0.06 to 1.25, the axial dispersion of flame is reduced, and the flame spreads more in the radial direction due to which axial velocity peak increases. At axial locations 0.05 m, the swirl strength doesn't have a significant effect on axial velocity from 0.06 m<R<0.2 m. At axial location

0.2 m, two peaks of axial velocity are obtained for swirl numbers of 0.06 and 0.57, whereas the single peak of axial velocity is obtained for swirl numbers 1 and 1.25.

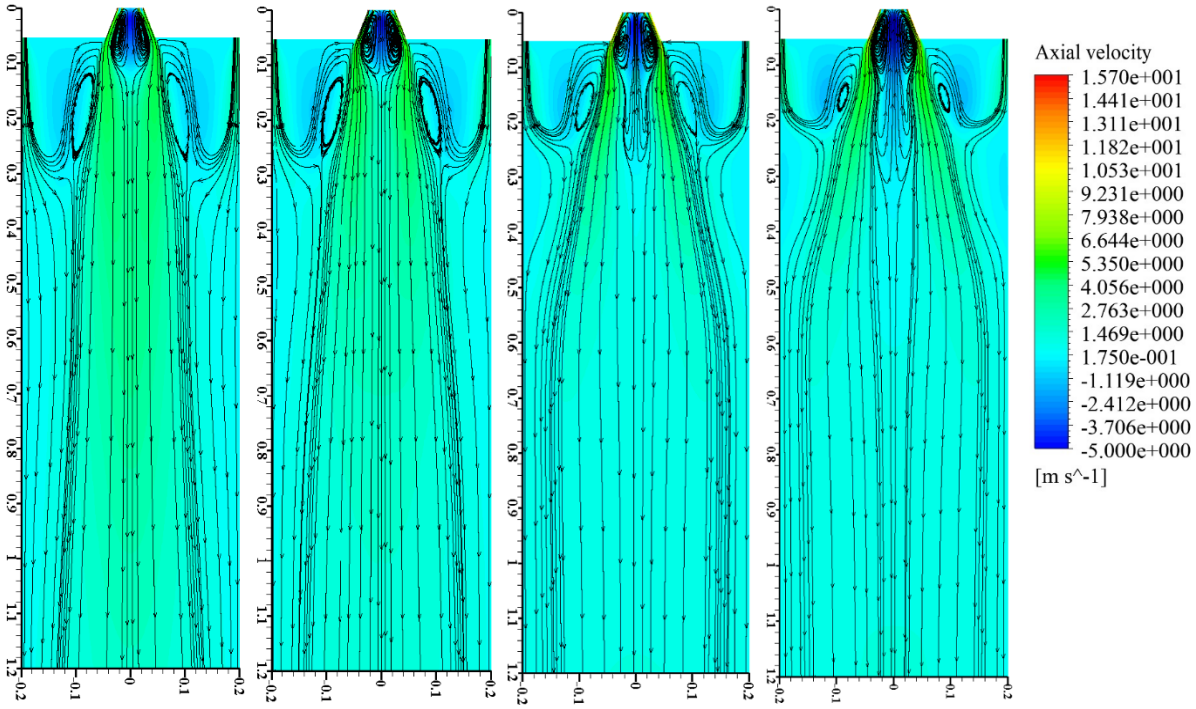

(a) **(b)** **(c)** **(d)**

Fig. 4.1. Axial velocity (m/s) contour for different swirl numbers **(a)** S=0.06 **(b)** S=0.57 **(c)** S=1.0 **(d)** S=1.25

Fig. 4.3 shows the radial variation of tangential velocity for different swirl numbers at axial locations 0.05 m and 0.2 m from burner outlet. At axial location 0.05 m, the peak negative tangential velocity can be observed at a radial position 0.04 m for all the swirl numbers. The peak tangential velocity decays sharply then almost become constant. At axial locations 0.2 m from burner outlet, the effect of swirl is not as prominent as it was for axial location 0.05 m.

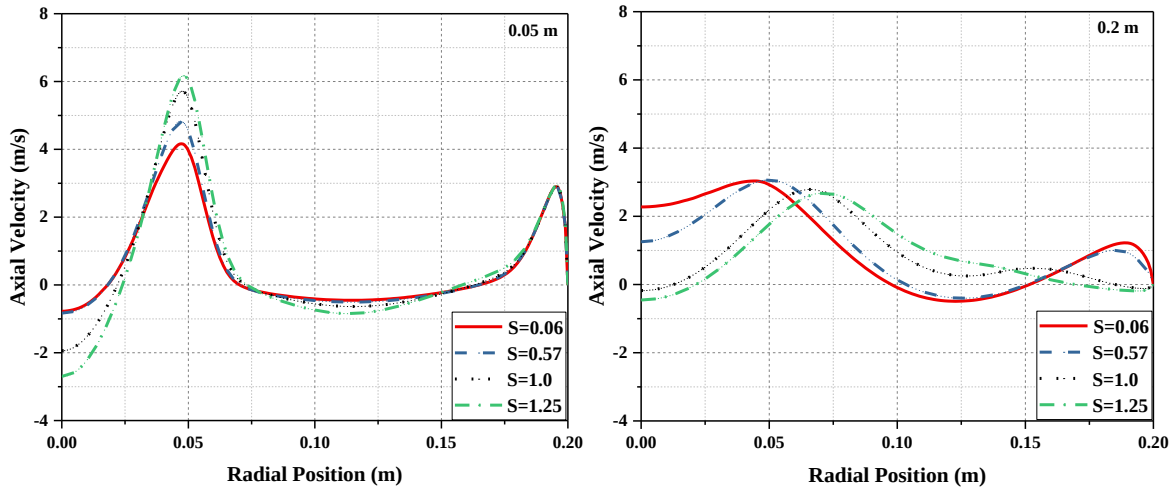

(a) **(b)**

Fig. 4.2. Radial variation of axial velocity (m/s) for different swirl number at axial location **(a)** 0.05 m and **(b)** 0.2 m

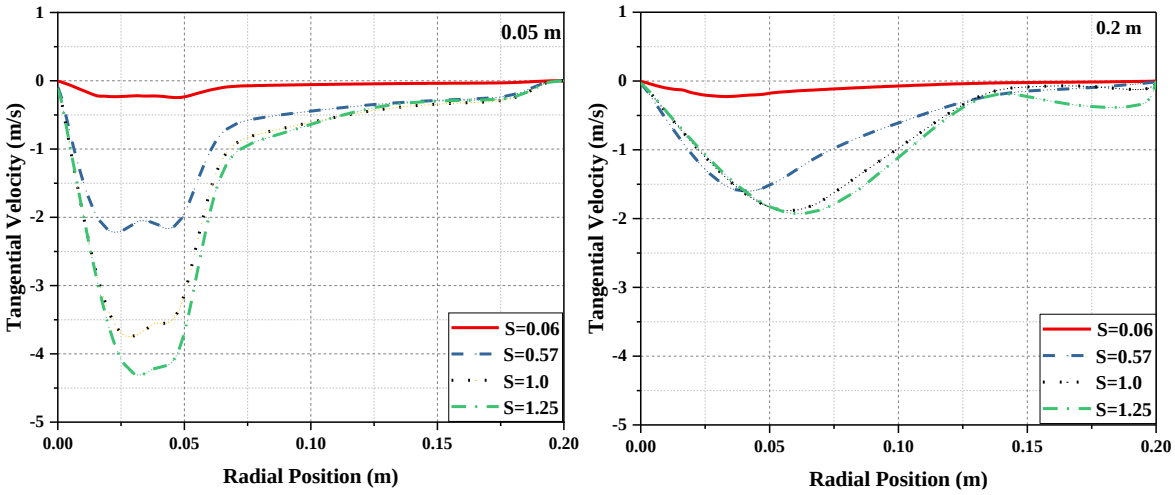

(a) **(b)**

Fig. 4.3. Radial variation of tangential velocity (m/s) for different swirl number at axial location **(a)** 0.05 m and **(b)** 0.2 m

4.2.2 Temperature Distribution

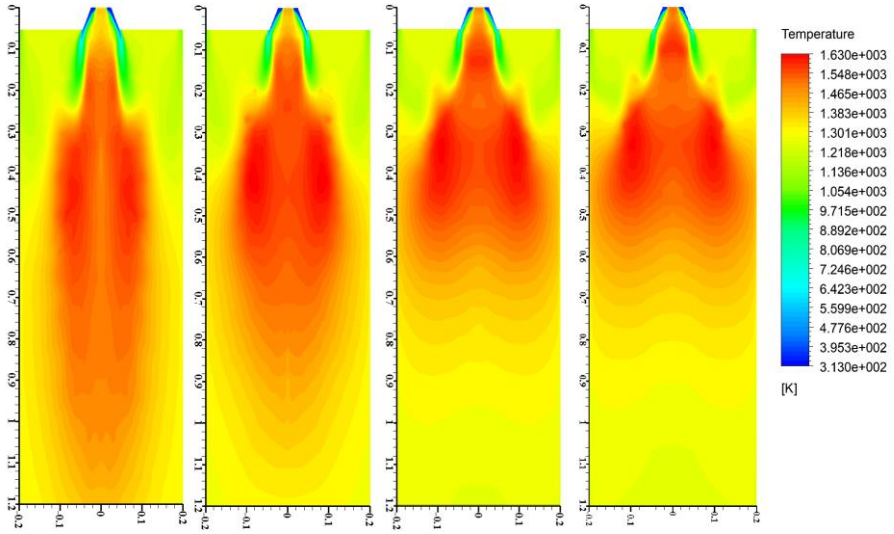

(a) **(b)** **(c)** **(d)**

Fig. 4.4. Contour of temperature (K) distribution for different swirl numbers **(a)** S=0.06 **(b)** S=0.57 **(c)** S=1.0 **(d)** S=1.25

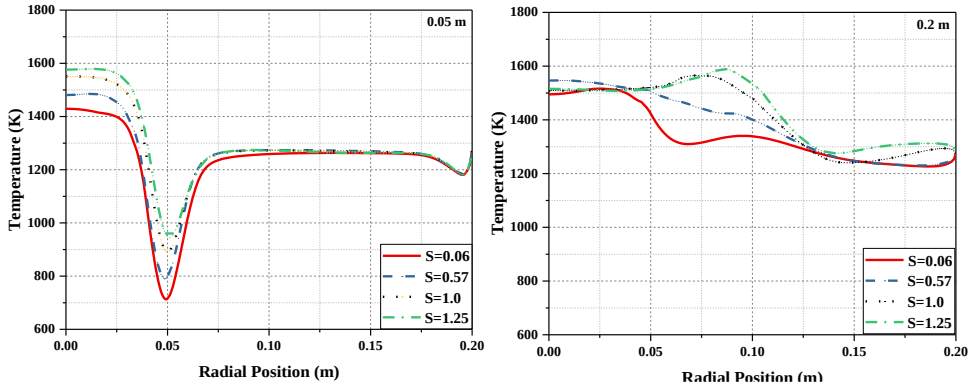

(a) **(b)**

Fig. 4.5. Radial variation of temperature (K) for different swirl number at axial location **(a)** 0.05 m and **(b)** 0.2 m

The temperature contour for different swirl number is shown in Fig. 4.4. Swirl strength strongly influenced the shape of the flame formed. At swirl number S=0.06, longer flame front is obtained in the investigation. As the swirl number is increased flame spread out more radially and prolonged flame began to be shorter. More intense and stable flames are obtained at higher swirl strength due to enhanced mixing of fuel and oxidizer streams.

Almost similar temperature distribution inside the combustor is observed, by increasing swirl number from 1.0 to 1.25.

Fig. 4.5 shows the radial variation of gas temperature at axial locations 0.05 and 0.2 m for different swirl numbers. With an increase in swirl strength, we obtained highly radial dispersed shorter flame due to spreading of the secondary stream. At axial location 0.05 m, minima of temperature obtained. The minimum temperature obtained at radial position 0.05 m increases with increase in swirl number. Radial temperature profile is not affected by swirl strength in region (0.07<R<0.2 m). At axial location 0.2 m, peak temperature shifts towards the radial direction with an increase in the swirl strength.

4.3 Effect of Various Combustion Environment

The combustion characteristics under oxy-coal (O_2/CO_2) atmosphere is highly influenced by the different thermo-physical properties of CO_2 compared to N_2. Flame temperature under O_2/CO_2 combustion atmosphere is significantly reduced when keeping the O_2 content similar to the O_2 content of the air. This is accompanied by delayed ignition and decelerated devolatilization and may lead to difficulties in stabilizing the flame for burners not optimized for oxy-fuel combustion. In order to improve the stability of these coal flames in oxyfuel atmosphere, the O_2 content of the oxidizer has to be increased up to 25 vol% and in some cases even up to 30 vol%. The oxygen concentration in oxy-fuel combustion is variable and therefore holds the possibility to meet desired conditions in terms of combustion and heat transfer by changing the O_2 concentration in the oxidizer. Thus, in this section, a comparative analysis of four different combustion environment obtained by varying the O_2 concentration in the feed gas has been presented.

4.3.1 Flow Field Distribution

The contour of axial velocity for four different combustion environment is shown in Fig. 4.6. From the figure, it can be interpreted that with an increase in O_2 concentration, the radial and axial dispersion of the internal recirculation zone is suppressed. The shape of velocity contours under different combustion environment is somewhat similar. The two external recirculation zones are created in all four combustion environment investigated in the study. The shape of the external recirculation zone slightly shrinks with an increase in O_2 concentration in CO_2.

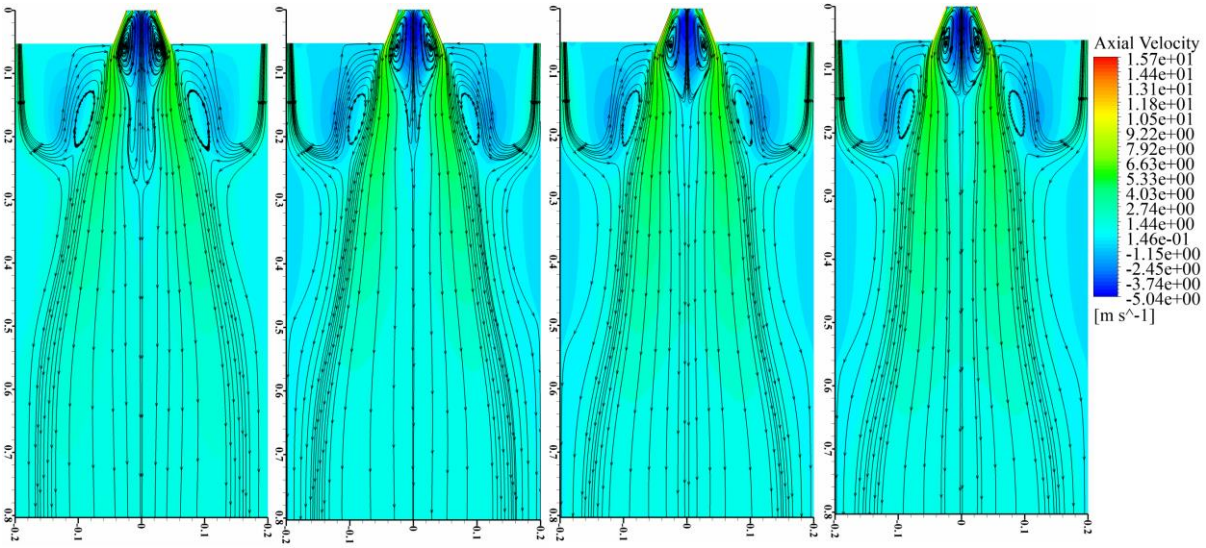

(a) **(b)** **(c)** **(d)**

Fig. 4.6. Contour of axial velocity (m/s) under different combustion conditions **(a)** 21% O_2/79% CO_2 **(b)** 25% O_2/75% CO_2 **(c)** 30% O_2/70% CO_2 **(d)** 35% O_2/65% CO_2

4.3.2 Temperature Distribution

Fig. 4.7 shows the temperature contour under different combustion environment obtained by changing the concentration of O_2 and CO_2 in the oxidizer. From the contour, it can be

seen that by increasing concentration of O_2 in the oxidizer, flame temperature rises and flames tend to be narrower. As the O_2 concentration in the O_2/CO_2 feed gas is increased, the ignition position of pulverized coal particles shifts near the burner due to the increased flame temperature at higher O_2 concentration. The flame temperature of oxy-21% O_2 is around 300 K lower than the oxy-35% O_2. The flame length is reduced with an increase in O_2 content in oxidizer due to faster ignition of coal particles under enriched O_2 level. The change of flame shape in four cases investigated can easily be seen. Oxy-21% O_2 combustion case has produced the longest flame front, whereas Oxy-35% O_2 combustion case has produced the shortest flame. From Fig. 4.7, it can be concluded that with an increase in O_2 concentration in the feed gas, flame diminishes in both axial and radial direction due to shifting of ignition position near to burner at high flame temperature.

Fig. 4.8 shows the radial variation of flame temperature in various combustion environments obtained by varying the composition of feed gas. At axial location 0.05 m from burner outlet, the variation of flame temperature is observed at radial position ($0<R<0.05$ m). Almost identical temperature profile is obtained at a radial position ($0.05<R<0.2$ m) in the various combustion environment investigated in the study. The corresponding level of temperature minima obtained also rises with an increase in O_2 concentration in the feed gas. At axial locations 0.2 m from burner exit, the position of peak temperature shifts in the radial direction. Slight variation in gas temperature profile is observed at the outer radial location which was absent at axial location 0.05 m from the burner exit. As the O_2 content in the feed gas is increased, the shape of flame becomes more confined and shifts toward burner with higher flame temperature in this zone. It

causes an increase in oxygen content near the reaction zone of the burner. Furthermore, less amount of CO_2 will absorb less amount of heat generated by combustion reaction. Thus, the flame temperature rises under the combustion environment having high O_2 concentration.

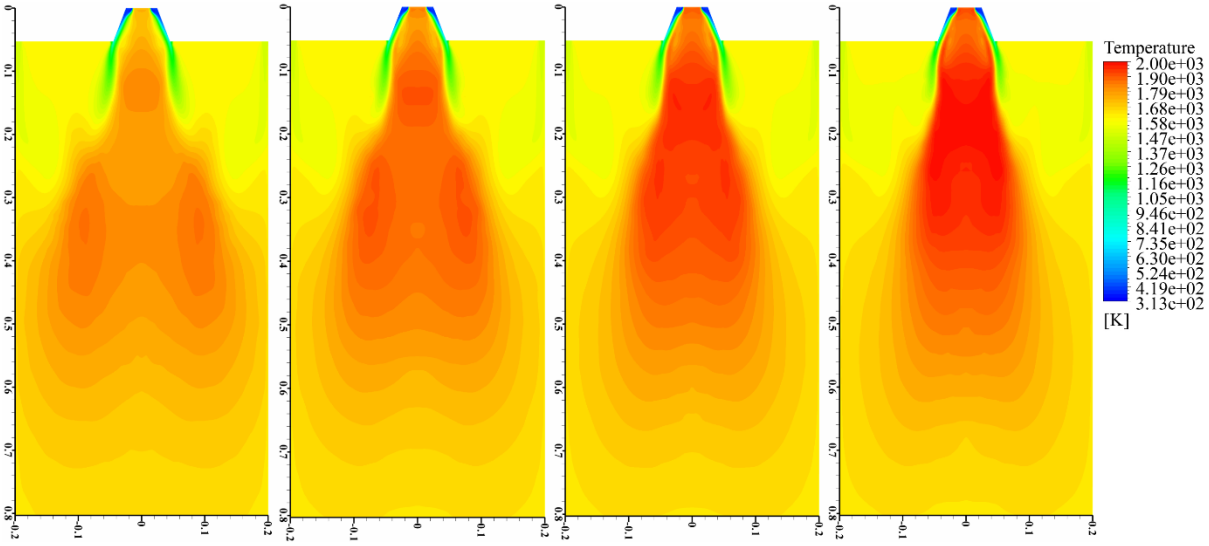

(a) **(b)** **(c)** **(d)**

Fig. 4.7. Contour of temperature (K) under different combustion conditions **(a)** 21% O_2/79% CO_2 **(b)** 25% O_2/75% CO_2 **(c)** 30% O_2/70% CO_2 **(d)** 35% O_2/65% CO_2

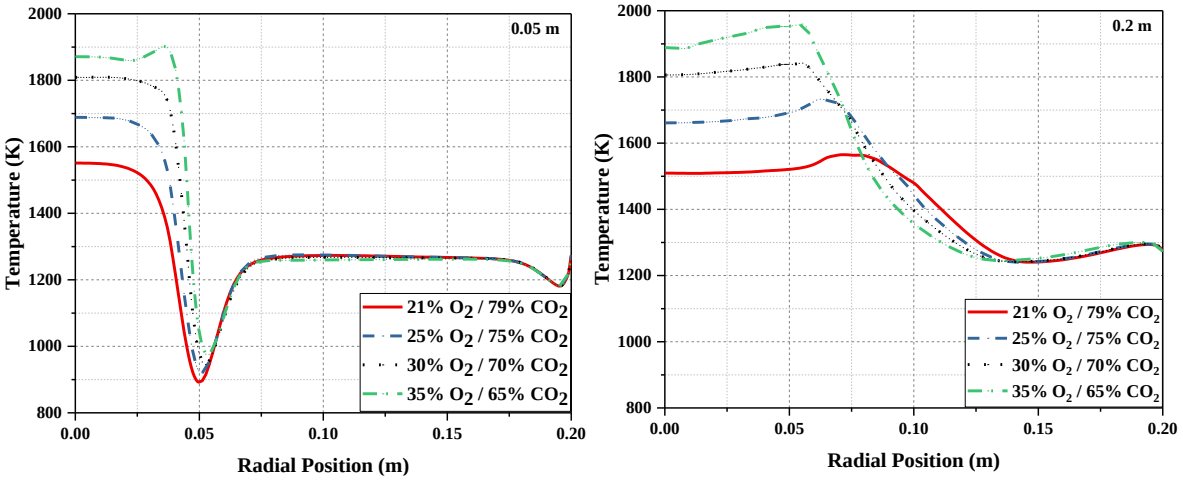

(a) **(b)**

Fig. 4.8. Radial variation of gas temperature (K) under different combustion environment at axial locations **(a)** 0.05 m and **(b)** 0.2 m.

4.3.3 Distribution of Char Burning Rate and Oxygen mole fraction

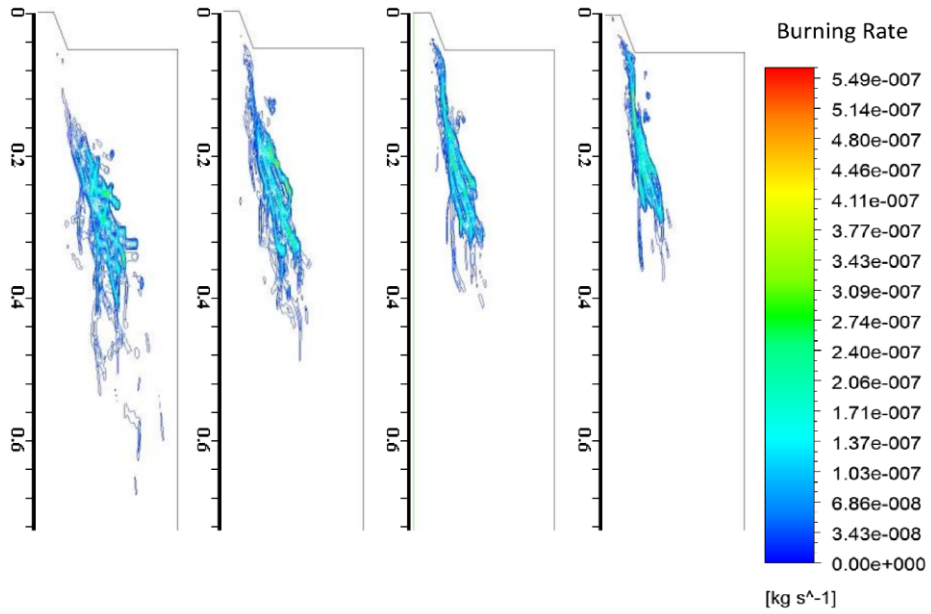

(a) **(b)** **(c)** **(d)**

Fig. 4.9. Predicted char burning rate inside combustion chamber under **(a)** oxy-21 **(b)** oxy-25 **(c)** oxy-30 and **(d)** oxy-35 combustion conditions

The distribution of predicted char burning rate (kg/s) and oxygen mole fraction inside the combustion chamber in different combustion conditions is shown in Fig. 4.9 and Fig. 4.10 respectively. An increase in O_2 concentration in the oxy-fuel atmosphere has resulted in increased temperature, burning rate and oxygen consumption. The devolatilization and combustion phenomenon of coal particles get enhanced with increasing O_2 concentration in oxy-fuel combustion conditions as excess oxygen promotes the volatiles consumption rate and provide extra heat to coal particles. The predicted temperature is strongly dependent on oxygen consumption and char burning rate. Therefore, as it can be seen in Fig. 4.9, the burning rate enhances with an increase in oxygen concentration, leading to increased oxygen consumption (Fig. 4.10). With an increase in oxygen concentration, the ignition

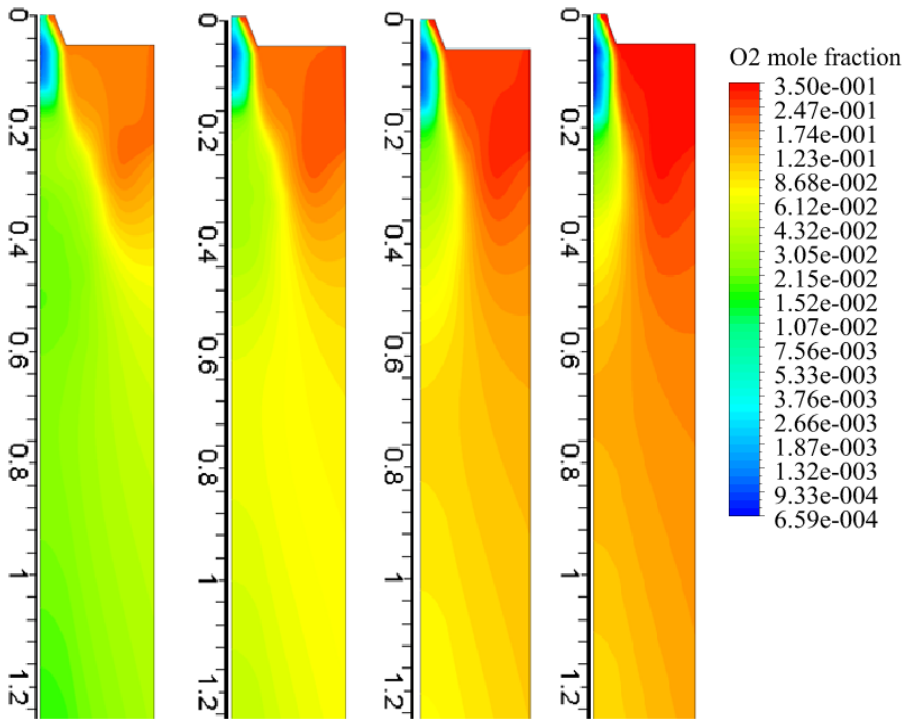

(a) **(b)** **(c)** **(d)**

Fig. 4.10. Predicted oxygen mole fraction inside combustion chamber under **(a)** oxy-21 **(b)** oxy-25 **(c)** oxy-30 and **(d)** oxy-35 combustion conditions

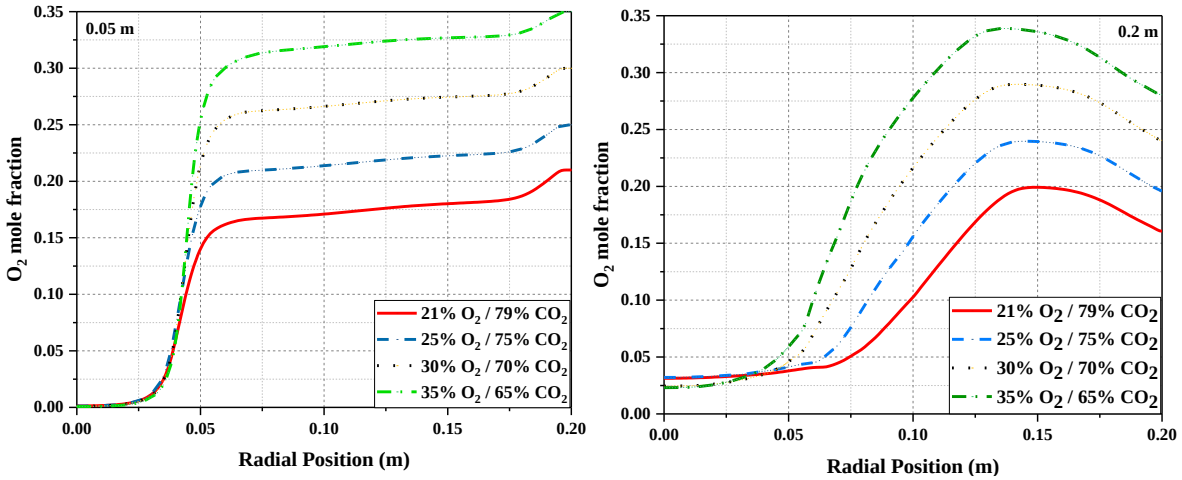

(a) **(b)**

Fig. 4.11. Radial variation of O_2 mole fraction under different combustion environment at axial locations **(a)** 0.05 m and **(b)** 0.2 m

zone shifts toward the burner, hence higher temperature and earlier initiation of char combustion can be seen in Fig. 4.7 and Fig. 4.9, respectively. The peak temperature obtained in oxy-25, oxy-30 and oxy-35 oxy-coal combustion cases are 107 K, 248 K and 357 K higher than the oxy-21 combustion case.

Fig. 4.11 displays radial profile of O_2 mole fraction for different oxygen concentrations at axial locations 0.05 m and 0.2 m from the burner exit. Oxygen consumption near the burner region has a vital influence on fuel consumption and flame characteristics in oxy-fuel combustion conditions. At axial location 0.05 m, the variation of O_2 is insignificant at radial position (0< R<0.04 m). The radial position (0< R<0.04 m) represent the flame front region in which the maximum temperature of the corresponding combustion case is obtained. Thus, most of the oxygen is consumed in this region. At radial position (0.05< R<0.2 m), the oxy-coal combustion case having higher O_2 concentration shows higher O_2 mole fraction. At axial location 0.2 m, radial profile of O_2 mole fraction is almost identical up to radial position 0.04 m. At radial position (0.04<R<0.2 m), oxy-coal combustion case having higher oxygen concentration shows higher O_2 mole fraction.

4.3.4 Comparison of Temperature and Radiation under Air-Fired and Oxy-Fired Combustion

Fig. 4.12 shows the axial profile of the gas temperature of air and four oxy-fuel combustion cases. The oxy-fuel combustion cases are obtained by varying O_2 and CO_2 concentration in the oxidizer. From Fig. 4.12, it is evident that the gas temperature is lower in the oxy-fuel case than the air-fired case at identical O_2 concentration. As CO_2 has higher heat capacity

than N_2; thus, CO_2 works as a better heat sink than N_2 and flame temperature reduces in oxy-fuel case having identical O_2 content. To obtain the peak temperature that was obtained in air-fired combustion, the O_2 content must be increased to around 30%. The temperature peak in oxy-fuel cases is obtained closer to burner than the air-fired case due to initiation of char combustion earlier in oxy-fired cases. Oxy-21 has two peaks of gas temperature, whereas the other three oxy-fuel cases have a single peak. The peak temperature of oxy-fired combustion increases with an increase in oxygen content in the oxidizer. As the oxygen content in the oxidizer is increased, the local stoichiometry rises, resulting in enhanced reaction kinetics and burning rate. This is the major reason behind the increase in gas temperature and oxygen consumption rate. The peak temperature obtained in oxy-25, oxy-30 and oxy-35 cases is around 10%, 18% and 24% higher than the oxy-21 case. The effect of combustion environment on gas temperature profile is almost negligible after axial location 0.65 m from the burner. With an increase in the oxygen content, the combustion location shifts towards the burner, hence a sudden rise in gas temperature profile is obtained at the burner exit.

The variation of surface incident radiation along the wall of the combustor is shown in Fig. 4.13. The accurate prediction of surface incident radiation is strongly dependent on the correct prediction of the temperature field inside the combustion chamber as heat transfer by radiation is proportional to the fourth power of the temperature. Fig. 4.13 shows the surface incident radiation is in range of 340-435 kW/m^2 for air-fired combustion. In contrast, the range of surface incident radiation for oxy-21, oxy-25, oxy-30 and oxy-35

cases have 195-260 kW/m^2, 265-335 kW/m^2, 310-420 kW/m^2 and 350-535 kW/m^2 respectively.

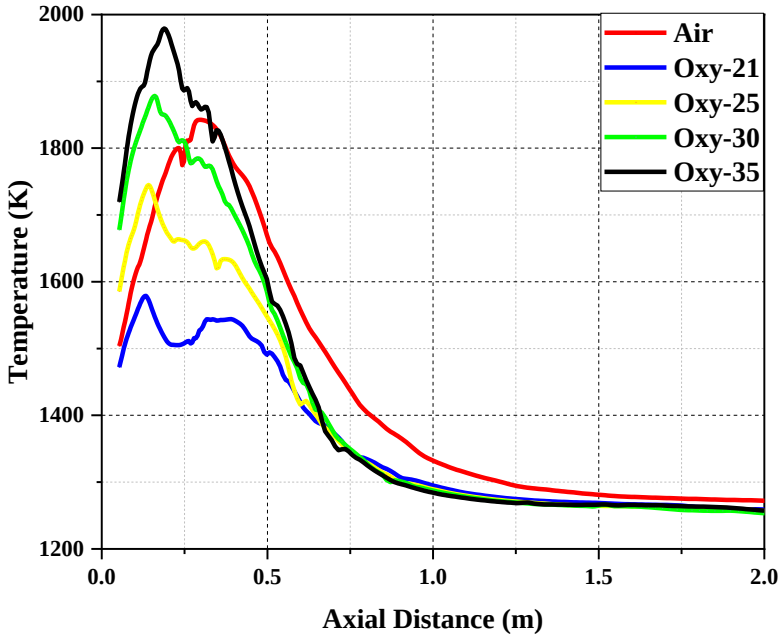

Fig. 4.12. Axial variation of gas temperature (K) for various combustion cases

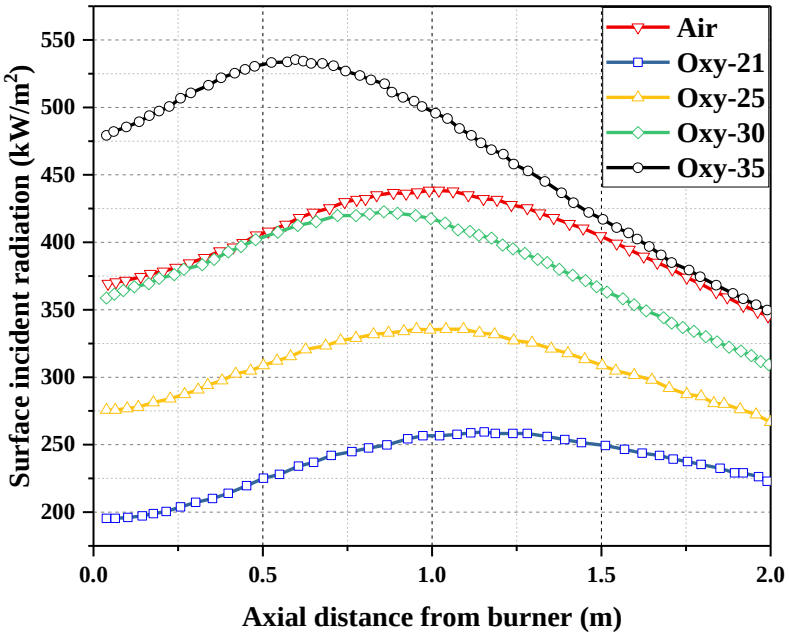

Fig. 4.13. Axial variation of surface incident radiation (kW/m^2) along the lateral wall from burner for various combustion case

To retrofit convention air-fired boiler to work under oxy-fired condition, the radiation intensities should be comparable. The oxy-30 case has somewhat similar surface incident radiation as obtained under air-fired combustion. From Fig. 4.13, it is evident that with an increase in O_2 content in oxy-fuel cases, surface incident radiation increases. When the O_2 content is increased in oxy-fuel cases, combustion takes place under enriched O_2 and less CO_2 combustion environment. Due to a decrease in CO_2 content, the specific heat of flue gas reduces, resulting in higher temperature and surface incident radiation.

4.3.5 Temporal Variations of Particle Phase Variables

Fig. 4.14 (a) represents the temporal history of particle volatile mass fraction obtained for particle sizes of 28, 55.2 and 95.9 µm under oxy-coal combustion atmosphere having 21% O_2 in the oxidizer. The temporal history provides information about particle ignition and devolatilization completion time. The volatiles are evolved during the devolatilization process of coal combustion. Devolatilization process is the fastest process of coal combustion, and it completes in the scale of milliseconds as shown in Fig. 4.14 (a). The particle class of 95.9 µm takes the longest time to deplete than the other particle classes. Fig. 4.14 (b) compares the temporal history of particle volatile mass fraction of fixed particle size of 95.9 µm in a various oxy-coal combustion atmosphere. From Fig. 4.14 (b), it can be seen that the particle depletion time reduces with an increase in oxygen concentration. The particles mass depletion is strongly dependent on its penetration into higher temperature region and its residence time in the combustor. With an increase in

oxygen content in oxidizer, the local stoichiometry near the burner enhances and results in reduced residence time.

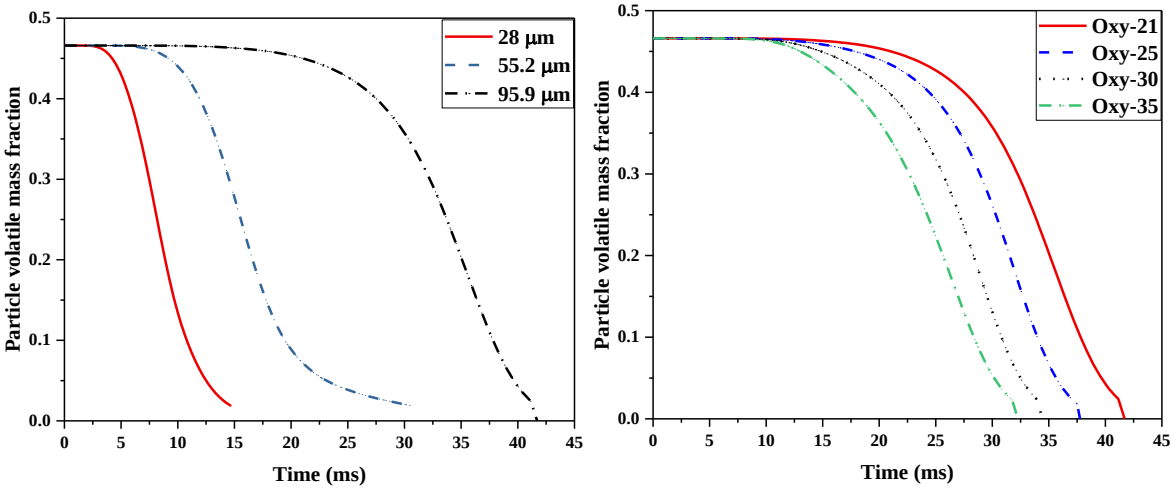

Fig. 4.14. Temporal history of particle volatile mass fraction for **(a)** different particle sizes under oxy-21 combustion atmosphere **(b)** 95.9 µm particle under various combustion atmosphere

Fig. 4.15 (a) shows the temporal history of particle char mass fraction for particle sizes of 28, 55.2 and 95.9 µm in oxy-coal combustion atmosphere having 21% O_2 in the oxidizer. From Fig. 4.15 (a), it is noted that the particles char mass fraction increases initially as during the devolatilization process the total mass flow rate of coal particle reduces due to release of volatile matter and in that period char mass remains constant. The peak char mass fraction is obtained when the total mass of volatiles is released, and char combustion initiates at this point. Char mass fraction starts reducing due to char combustion. Temporal mass history of the 95.9 µm particle is compared in various oxy-fuel combustion environment in Fig. 4.15 (b). As oxygen content in oxidizer is increased, the flame front region having maximum temperature shifted towards the burner, thus, enhancing the char

burnout rate. This results in the consumption of char earlier with an increase in oxygen content. Char consumption time reduces by around 63%, 75% and 80% in oxy-25, oxy-30 and oxy-35 respectively than the oxy-21 case.

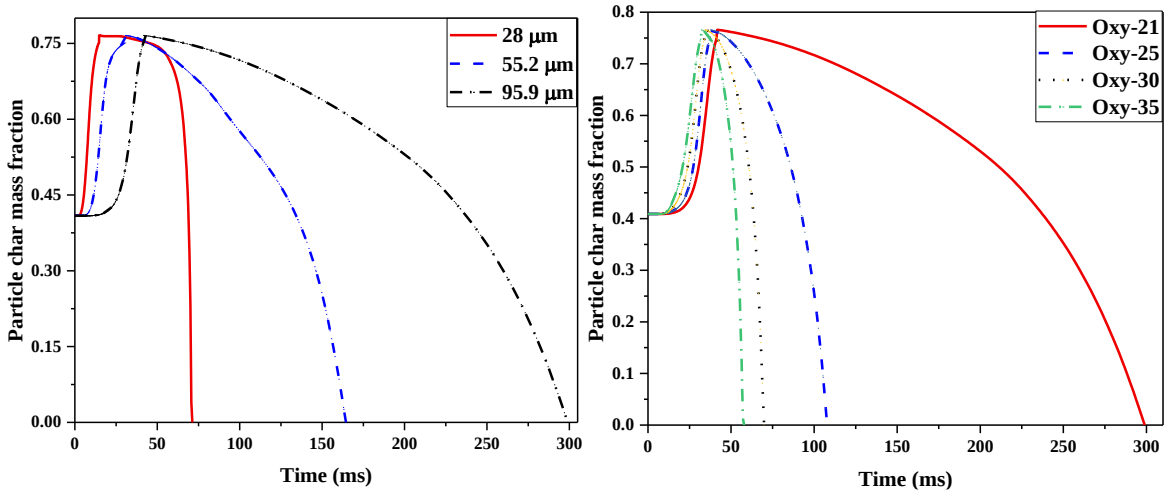

(a) **(b)**

Fig. 4.15. Temporal history of particle char mass fraction for **(a)** different particle sizes under oxy-21 combustion atmosphere **(b)** 95.9 µm particle under various combustion atmosphere

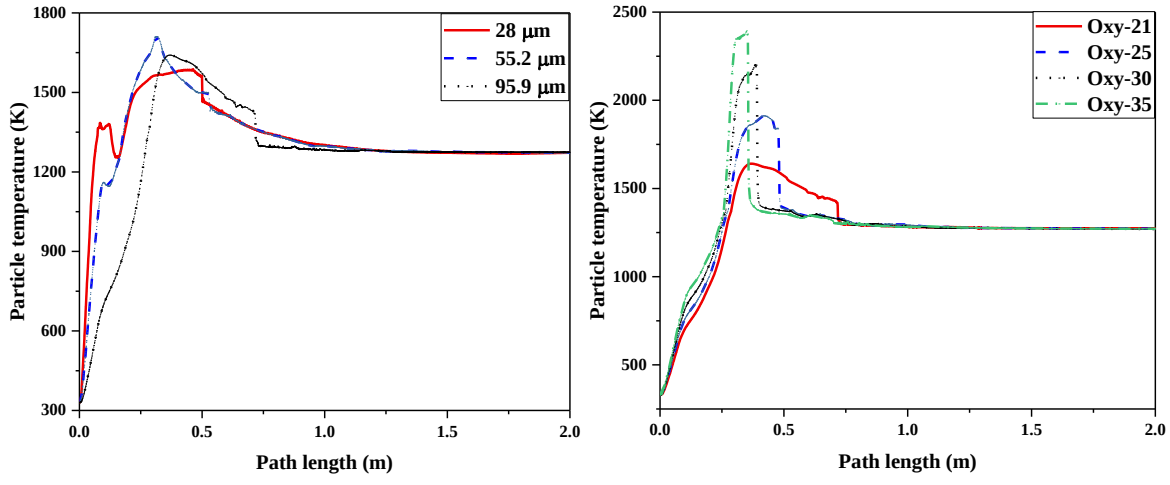

(a) **(b)**

Fig. 4.16. Variation of particle temperature history for **(a)** different particle sizes under oxy-21 combustion atmosphere **(b)** 95.9 µm particle under various combustion atmosphere

Fig. 4.16 (a) shows the variation of particle temperature history for particle sizes of 28, 55.2 and 95.9 μm in oxy-fuel combustion condition having 21% O_2 in the oxidizer. The particles undergo rapid heating in the initial period and attain peak temperatures. As the particle size is increased, the time required for volatile release and char consumption increases. Thus, the particle class of higher diameter attain peak temperature at a longer distance in the combustion chamber compared to particles of lower diameter. Fig. 4.16 (b) compares the particle temperature history of a fixed particle class of 95.9 μm diameter in various oxy-fuel combustion conditions. Oxy-35 combustion case has the highest peak temperature whereas oxy-21 combustion case has the lowest peak temperature. The broader peak obtained in oxy-21 combustion case tends to become narrow, and oxy-35 combustion case produces the narrowest peak. Peak particle temperature is 15%, 31% and 45% higher in oxy-25, oxy-30 and oxy-35 combustion case than the oxy-21 combustion case.

4.4 Effect of Inlet Feed Gas Temperature

Under this section, the effect of varying feed gas inlet temperature on the flow field and combustion characteristics under oxy-fuel combustion condition has been discussed. Three cases having different inlet feed gas temperatures have been investigated. The feed gas inlet temperatures of the primary, secondary and tertiary stream are varied, whereas inlet temperature of the staging stream is kept constant. The flow rate of feed gas through the inlet openings is kept constant while changing its inlet temperature. All the investigations have been performed under base oxy-fuel combustion environment (S=1) for which experimental validation has been discussed.

4.4.1 Flow Field Distribution

The axial velocity contour for the different inlet temperature of the feed gas is shown in Fig. 4.17. As the temperature of the feed gas is increased keeping its flow rate constant, the density of feed gas reduces and results in higher axial velocity. Both strength and axial dispersion of the internal recirculation zone is greater at higher inlet temperature.

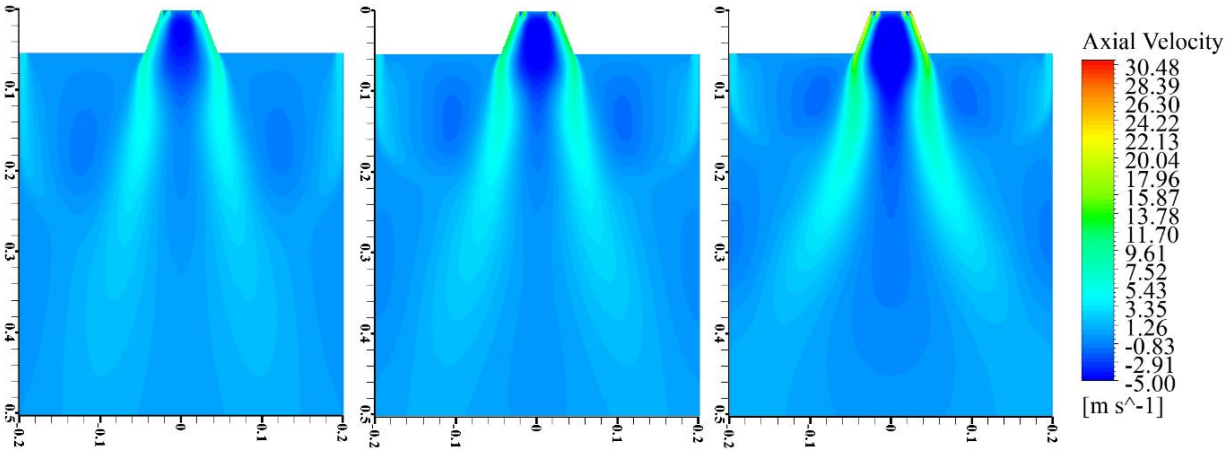

(a) **(b)** **(c)**

Fig. 4.17. Contour of axial velocity (m/s) for different inlet feed gas temperatures **(a)** 313 K **(b)** 500 K and **(c)** 800 K

Fig. 4.18 shows the radial variation of axial velocity for the different inlet temperature of feed gas at axial locations 0.05 and 0.2 m from burner exit. From Fig. 4.18, it is visible that as the inlet temperature of the feed gas is increased, peak axial velocity increases. At axial location 0.05 m, peak axial velocity increases by 27% and 70% when inlet temperature of feed gas is increased to 500 K and 800 K from the base case of 313 K. Stronger recirculation zone is created at the higher feed gas temperature. At axial location 0.2 m from the burner, the influence of the inlet temperature of the feed gas is marginal.

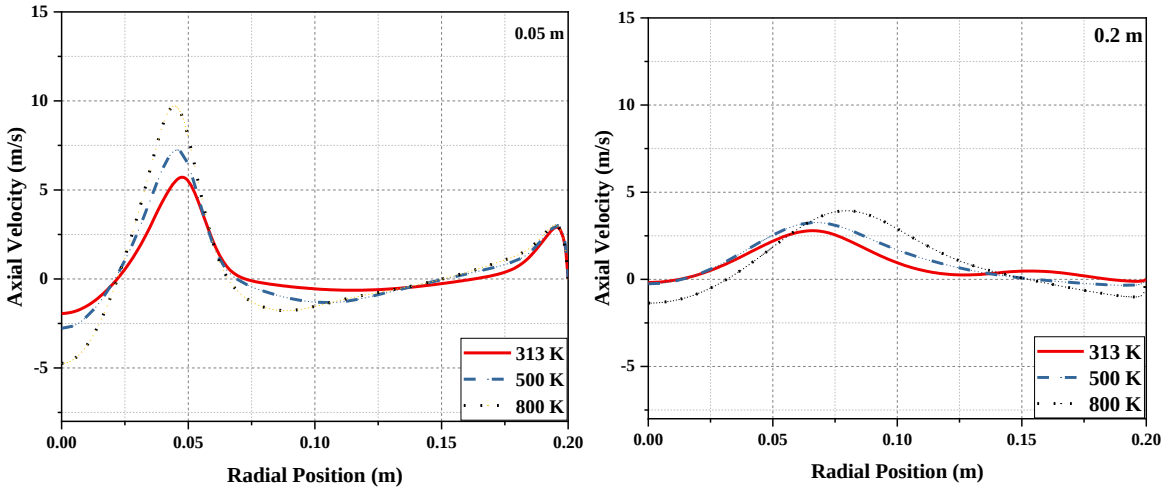

(a) **(b)**

Fig. 4.18. Radial variation of axial velocity (m/s) for different inlet feed gas temperatures at axial locations **(a)** 0.05 m and **(b)** 0.2m

4.4.2 Temperature Distribution

Fig. 4.19 shows the contour of gas temperature for the different inlet temperature of the feed gas. From the contour, it can be seen that with an increase in inlet temperature, the axial dispersion of flame is restricted and flame shifts toward near burner region. At higher inlet temperature, the combustion of volatile matter present in coal shifted near the burner region. So, the gas temperature is higher in that region at the higher inlet temperature.

The variation of flame temperature along the radial direction at axial locations 0.05 and 0.2 m from burner exit for different inlet feed gas temperature is shown in Fig. 4.20. The peak flame temperature predicted for inlet feed gas temperature 500 and 800 K is around 3% and 9% higher than the base case of feed gas temperature 313 K. At axial location 0.05 m, the minima of flame temperature rise to a higher value at higher inlet feed gas temperature. At axial location 0.2 m, the flame temperature is around 50-80 K higher for higher inlet feed

gas temperature throughout the radial direction, and the peak temperature is shifted in the radial direction.

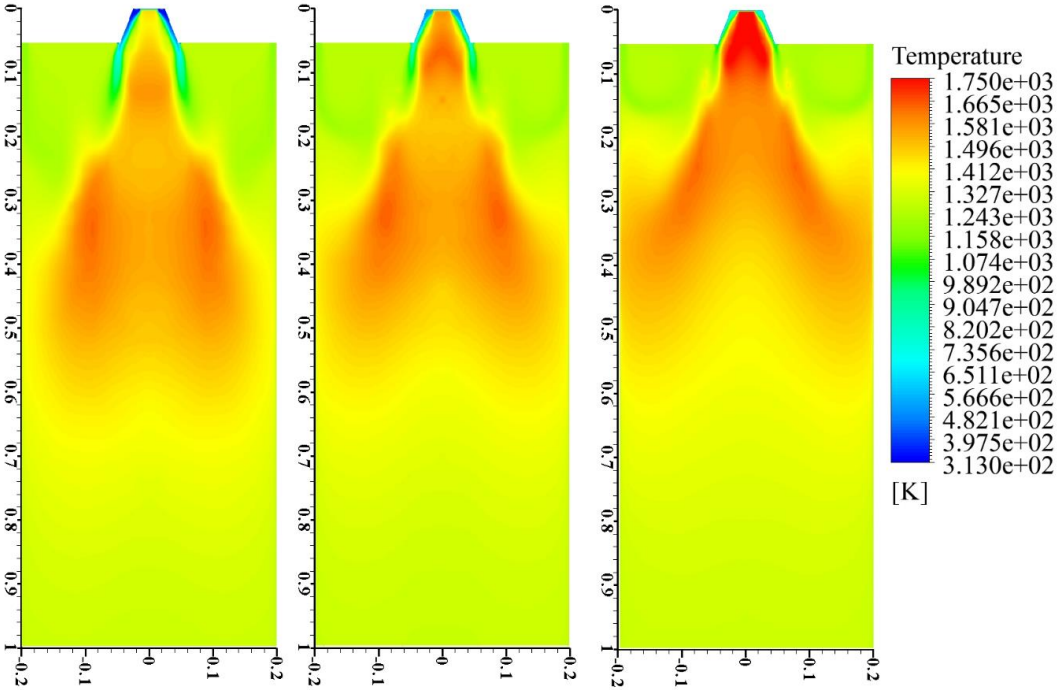

(a) **(b)** **(c)**

Fig. 4.19. Contour of temperature (K) for different inlet feed gas temperatures **(a)** 313 K **(b)** 500 K and **(c)** 800 K

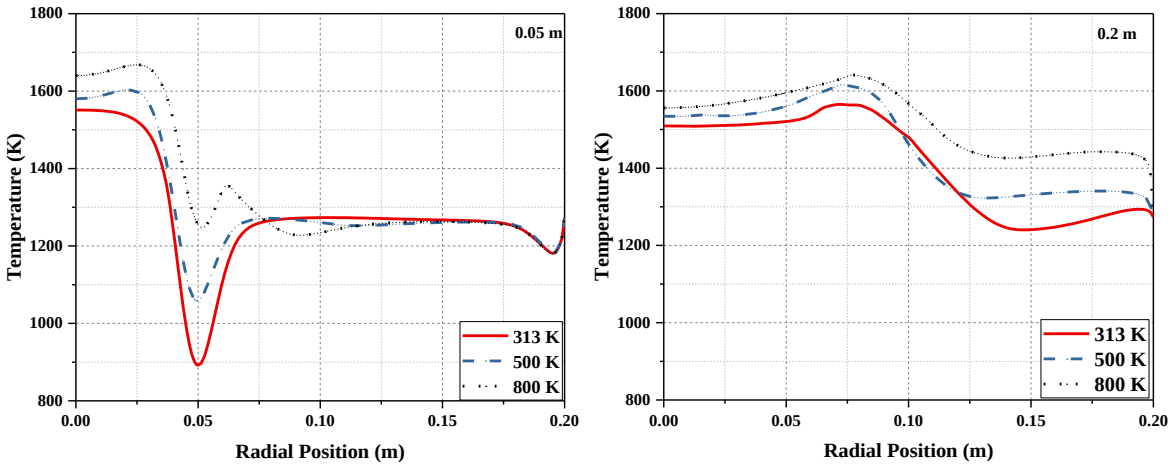

(a) **(b)**

Fig. 4.20. Radial variation of temperature (K) for different inlet feed gas temperatures at axial locations **(a)** 0.05 m and **(b)** 0.2 m

4.5 Effect of Inlet Feed Gas Pressure

Under this section, the effect of varying feed gas inlet pressure on the flow field and combustion characteristics under oxy-fuel combustion condition has been discussed. Three cases having different inlet feed gas pressure have been investigated. These feed gas inlet pressures are (a) 1.0 bar (base case) (b) 5.0 bar and (c) 10 bar. The flow rate of feed gas through the inlet openings is kept constant while changing its inlet pressure. All the investigations have been performed under base oxy-fuel combustion environment (S=1) for which experimental validation has been discussed.

4.5.1 Flow Field Distribution

The axial velocity contour for different values of inlet feed gas pressure, namely 1.0, 5.0 and 10 bar is shown in Fig. 4.21. As the mass flow rate of the feed gas is kept constant, with an increase in inlet feed gas pressure, the density increases, which ultimately results in reduced axial velocity. The reduced values of axial velocity can easily be seen in Fig. 4.21. The shape of the internal recirculation zone (IRZ) created along the axis near the burner, changes significantly with an increase in inlet feed gas pressure. At 1.0 bar pressure, very strong internal recirculation zone (IRZ) is created, and its strength decays with an increase in inlet feed gas pressure. The length of the flame front is also reduced with an increase in inlet pressure of feed gas.

The effect of inlet feed gas pressure on the radial profile of axial velocity is shown in Fig. 4.22. The peak axial velocity is very small for inlet feed gas pressure of 5.0 bar and 10 bar in compare to the base case of 1.0 bar. Higher density at higher pressure has resulted in

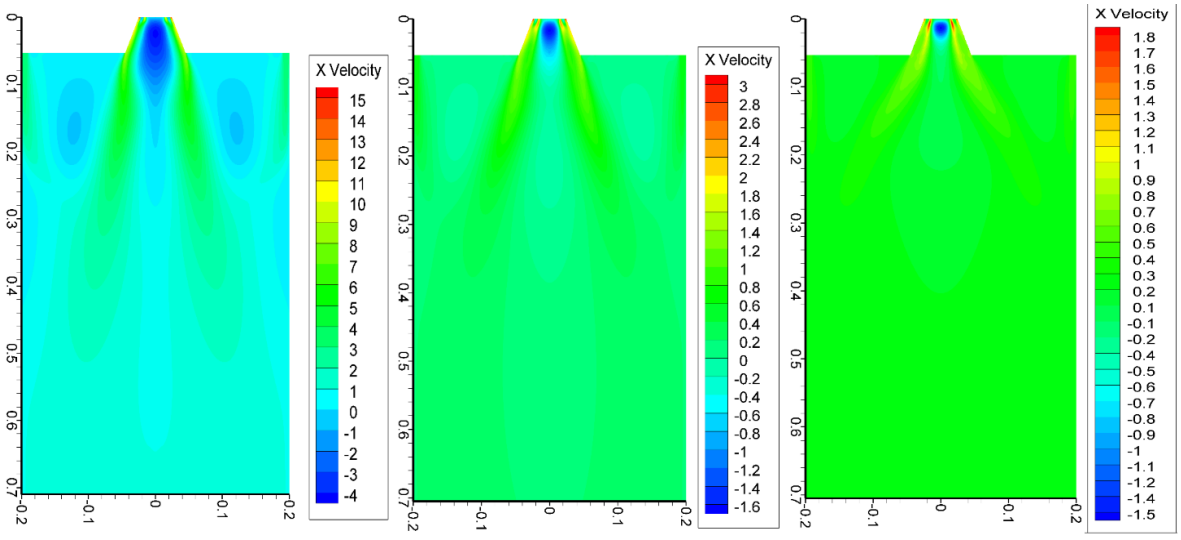

(a) **(b)** **(c)**

Fig. 4.21. Axial velocity (m/s) contour for different inlet feed gas pressures **(a)** 1.0 Bar **(b)** 5.0 Bar **(c)** 10 Bar

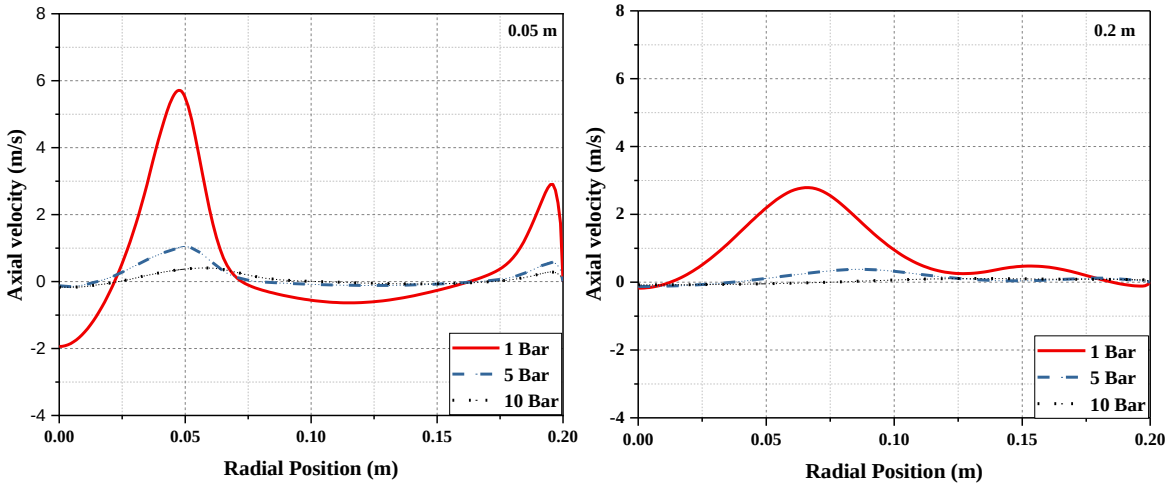

(a) **(b)**

Fig. 4.22. Radial variation of axial velocity (m/s) for different inlet pressures at axial locations **(a)** 0.05 m and **(b)** 0.2 m

lower axial velocity. At axial location 0.05 m from burner outlet, 5.0 and 10 bar inlet feed gas pressure combustion case have 80% and 90% reduction in peak axial velocity than the

base combustion case of 1 bar feed gas pressure. At axial locations 0.2 m, the peak of axial velocity is shifted in the radial direction.

4.5.2 Temperature Distribution

The effect of different inlet feed gas pressure on temperature contour is shown in Fig. 4.23. The structure of flame is altered significantly with an increase in feed gas inlet pressure. From gas temperature contour, it can be noted that the axial dispersion of flame is suppressed with an increase in inlet feed gas pressure. Under high pressure conditions, the drag force on particle comes into the picture and restrict the particle to move along the length of the combustor. The inlet feed gas pressure 5.0 and 10.0 bar have 16% and 32% reduction in flame length in comparison to the base case having 1.0 bar pressure. The effect of staging stream on the flame front is marginal in 10 bar inlet feed gas pressure, in comparison to the base case. The peak flame temperature is slightly higher in 10 bar inlet feed gas pressure condition.

The radial profile of gas temperature for different value of inlet feed gas pressures at axial locations 0.05 and 0.2 m is shown in Fig. 4.24. At axial location 0.05 m, the shape of the radial temperature profile is altered in the flame front region. The minima of temperature at a radial location around 0.05 m is obtained for 1.0 bar inlet feed gas pressure. The value of the minima temperature obtained is reduced and shifted slightly in the radial direction for 5.0 bar inlet feed gas pressure. Completely reverse nature of temperature profile is obtained at this radial location for 10.0 bar inlet feed gas pressure. The maxima of temperature is

found at this location. At axial location 0.2 m, the peak flame temperature is shifted radially outward with an increase in inlet feed gas pressure.

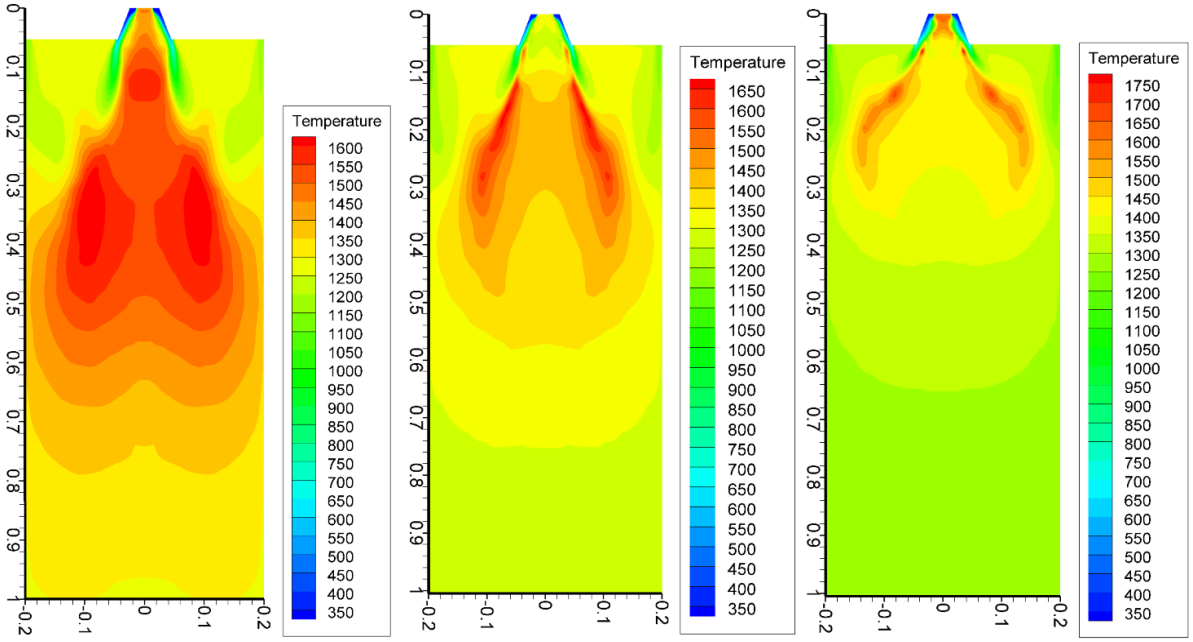

(a) **(b)** **(c)**

Fig. 4.23. Temperature contour (K) for different inlet feed gas pressures **(a)** 1 Bar **(b)** 5 Bar **(c)** 10 Bar

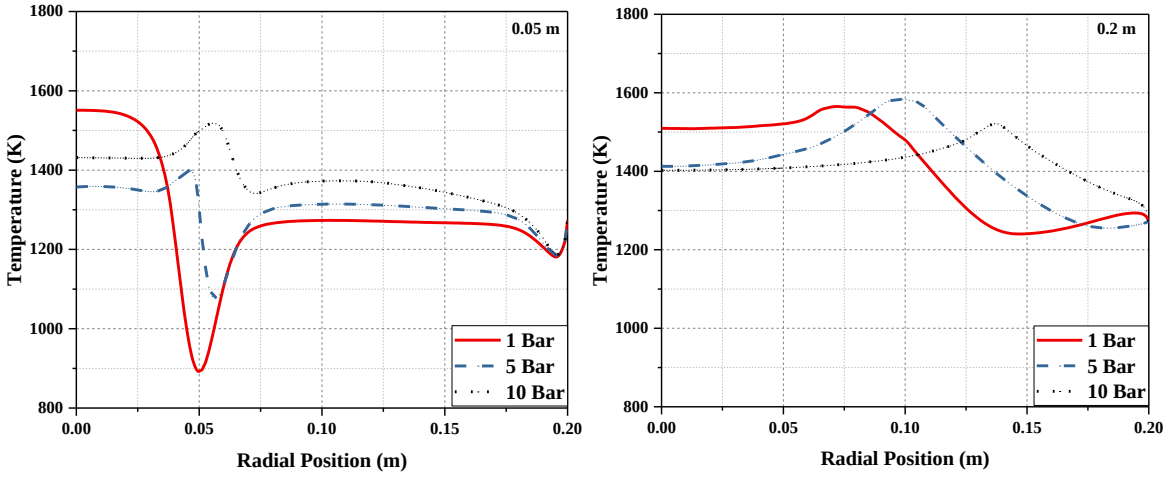

(a) **(b)**

Fig. 4.24. Radial variation of temperature (K) for different inlet pressures at axial locations **(a)** 0.05 m and **(b)** 0.2 m

4.6 Effect of Swirl Strength, Combustion Environment, Inlet Temperature and Pressure on Length of IRZ (m) and Flame Length (m)

The effect of swirl strength, combustion environment, inlet temperature and pressure of feed gas on the length of internal recirculation zone (IRZ) and flame length is shown in Fig. 4.25. The length of the internal recirculation zone (IRZ) is strongly affected by swirl strength, as shown in Fig. 4.25 (a). As the swirl strength increases, internal recirculation zone (IRZ) becomes more intense. The length of the flame front formed reduces with increase in swirl strength. The oxy-fuel combustion case having 21% O_2 in feed gas has the longest internal recirculation zone. As the O_2 content is increased, the length of the internal recirculation zone (IRZ) decreases. The increase of O_2 content from 30% to 35% has less impact on IRZ. The oxy-fuel combustion case having 35% O_2 in CO_2 has the shortest flame. With an increase in O_2 content in the oxidizer, ignition zone shifts near the burner due to high flame temperature and axial dispersion of flame reduces. The effect of inlet feed gas temperature on IRZ and flame length is shown in Fig. 4.25 (c). With an increase in the feed gas inlet temperature, longer IRZ is formed. Longest internal recirculation zone is observed for inlet feed gas temperature 800 K. The increase in the length of IRZ is greater for an increase in inlet feed gas temperature from 500 to 800 K than the corresponding increase in IRZ length for inlet feed gas temperature increase of 313 to 500 K. Flame length shortens at higher feed gas inlet temperature. The effect of inlet feed gas pressure on the internal recirculation zone and flame length is shown in Fig. 4.25 (d). The length of the internal recirculation zone increases with an increase in inlet feed gas pressure, but its

intensity decreases. At higher inlet feed gas pressures, the drag force on the particles increases, which ultimately results in shorter flames.

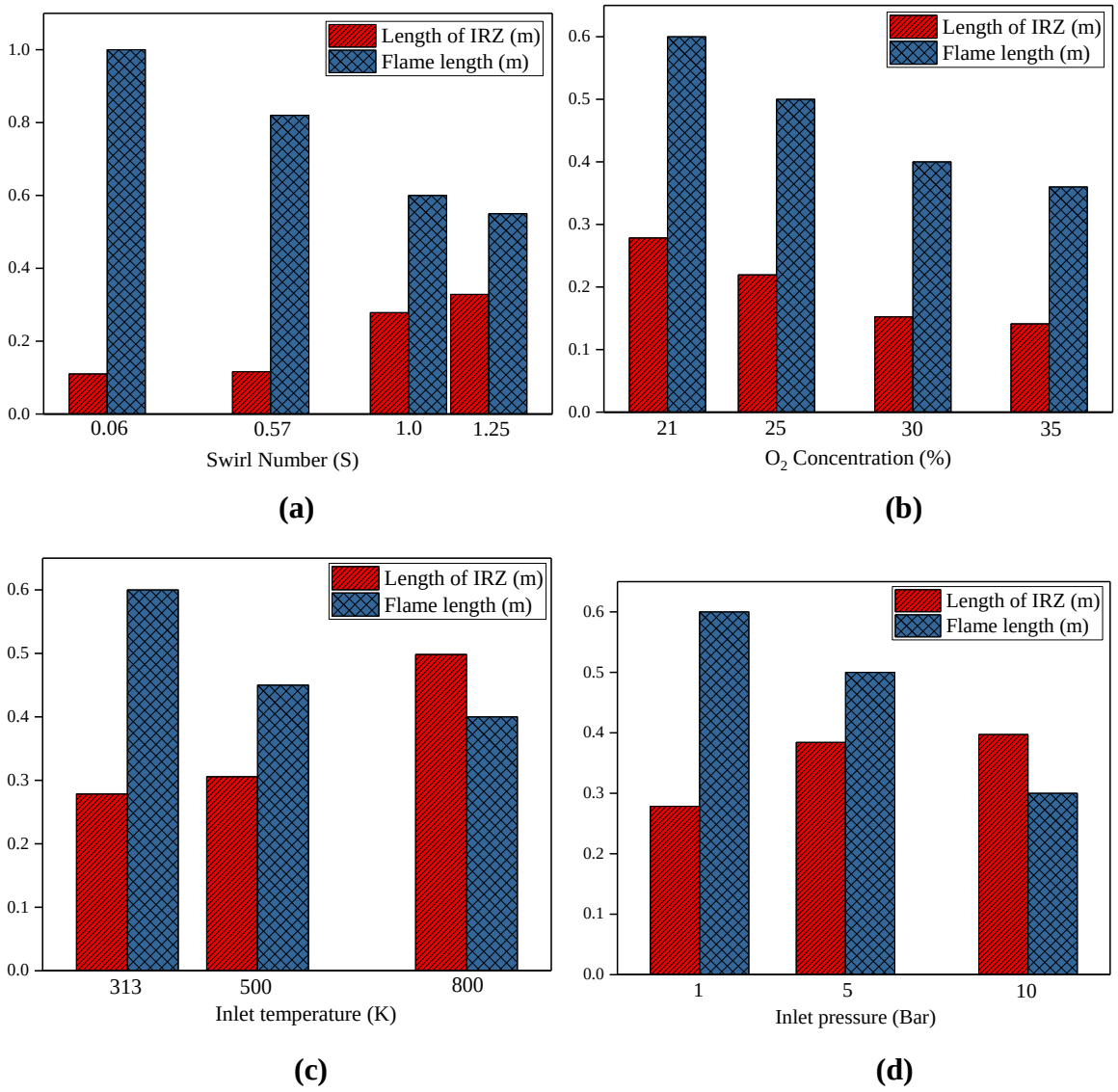

Fig. 4.25. The effect of swirl strength, combustion environment, inlet temperature and pressure of feed gas on length of IRZ (m) and flame length (m).

4.7 Summary

Based on the discussions held in this chapter, it can be summarized that the more intense and stable flame front has been observed at higher swirl number. At higher swirl number, the length of the internal recirculation zone (IRZ) enhances, whereas the size of the flame front diminishes. Based on the numerical results obtained by varying the composition of O_2/CO_2 in the oxidizer, it has been found that the ignition zone shifts towards the burner at higher O_2 concentration due to enhanced devolatilization and char combustion process, which ultimately resulted in increased flame temperature. The flame temperature and radiative heat transfer comparable to convention air-fired combustion atmosphere have been found at an oxygen concentration of 30% in oxy-coal combustion atmosphere. This chapter also demonstrated that the increase in both inlet temperature and pressure of feed gas resulted in shorter flame with higher flame temperature due earlier initiation of the combustion process.